Changes in photosynthetic electron transfer and state transitions in an herbicide-resistant D1 mutant from soybean cell cultures

Mercedes Roncel[a*], Inmaculada Yruela[b], Diana Kirilovsky[c], Fernando Guerrero[a], Miguel Alfonso[b], Rafael Picorel[b], José M. Ortega[a]

[a]Instituto de Bioquímica Vegetal y Fotosíntesis, Universidad de Sevilla-CSIC, Américo Vespucio 49, 41092-Sevilla, Spain. [b]Estación Experimental de Aula Dei, CSIC, Avda. Montañana 1005, 50059-Zaragoza, Spain. [c]Laboratoire de Bioénergétique Moléculaire et Photosynthèse, Institut de Biologie et Technologies-Saclay (iBiTec-S), CEA Saclay, 91191 Gif-sur-Yvette, France.

*Author for correspondence:

Mercedes Roncel

Instituto de Bioquímica Vegetal y Fotosíntesis, Universidad de Sevilla-CSIC, Américo Vespucio 49, 41092-Sevilla, Spain

Tel: 34 954 489525

Fax: 34 954 460065

E-mail: mroncel@us.es

Keywords: cyclic and linear electron flow; Photosystem I, Photosystem II, thermoluminescence; state transitions; D1 mutant

Abstract

Anomalies in photosynthetic activity of the soybean cell line STR7, carrying a single mutation (S268P) in the chloroplastic gene *psb*A that codes for the D1 protein of the photosystem II, have been examined using different spectroscopic techniques. Thermoluminescence emission experiments have shown important differences between STR7 mutant and wild type cells. The afterglow band induced by both white light flashes and far-red continuous illumination was downshifted by about 4ºC and the Q band was upshifted by 5ºC. High temperature thermoluminescence measurements suggested a higher level of lipid peroxidation in mutant thylakoid membranes. In addition, the reduction rate of $P700^+$ was significantly accelerated in STR7 suggesting that the mutation led to an activation of the photosystem I cyclic electron flow. Modulated fluorescence measurements performed at room temperature as well as fluorescence emission spectra at 77 K revealed that the STR7 mutant is defective in state transitions. Here, we discuss the hypothesis that activation of the cyclic electron flow in STR7 cells may be a mechanism to compensate the reduced activity of photosystem II caused by the mutation. We also propose that the impaired state transitions in the STR7 cells may be due to alterations in thylakoid membrane properties induced by a low content of unsaturated lipids.

Abbreviations: AG, afterglow (luminescence bounce); B band, TL band due to $S_{2/3}Q_B^-$ recombination; C band, TL band due to $Tyr_D^+Q_A^-$ recombination; FR, far-red light > 700 nm; HTL, high temperature thermoluminescence; PSI, photosystem I; PSII, photosystem II; Q band, TL band due to $S_2Q_A^-$ recombination; Q_A ,and Q_B, the primary and secondary quinone acceptors of the reaction centre of PSII; RC, reaction centre; S_2 and S_3, oxidized S^{2+} and S^{3+} states of the manganese oxygen-evolving complex of PSII, respectively; TL, thermoluminescence; t_{max}, temperature of the signal intensity maximum of a TL band

1. Introduction

The photosynthetic process operates according to two non-mutually exclusive modes in cyanobacteria, algae and plants: linear and cyclic electron flows. In the linear mode, electrons are transferred from water to NADP via the three major photosynthetic complexes, namely PSII, cytochrome b_6f and PSI. Cyclic electron flow driven by PSI produces ATP, but not NADPH. Several alternative electron pathways driven by PSI have been reported to recycle electrons towards the intersystem carriers, mediated by either the NAD(P)H dehydrogenase (NDH complex) or the putative ferredoxin:plastoquinone reductase (FQR complex) [1-4]. Environmental stresses, such as photoinhibition, high temperatures, drought or high salinity, stimulate the activity of alternative PSI-driven electron transports. Thus, these pathways may provide additional flexibility to respond to different environmental stresses in plants [1]. Recently, it has been demonstrated that both FQR and NDH complexes are involved in the electron transfer reactions leading to a thermoluminescence (TL) band emission named "afterglow" (AG) [5]. AG emission has been related to cyclic electron transport, since the addition of an inhibitor of this flow, antimycin, suppressed this process [6]. Moreover, it has been observed that short heat-treatments, in the same temperature range which induces AG emission, trigger a PSI-driven electron flow from reducing components of unknown identity in the stroma towards the acceptor side of PSII [7]. This supports the idea that AG emission is due to the heat-induced reduction of Q_B by a stromal component and further recombination with S_2/S_3 states of the manganese cluster in PSII [8-10].

State transitions have been described as an adaptation mechanism that allows plants and algae to respond to changes in the spectral quality of light by varying the relative absorption cross-section of PSI and PSII [11,12]. This mechanism involves the reversible association of the major antenna complex (LHCII) with either PSII (in state 1) or PSI (in state 2) depending on the redox state of the intersystem electron carriers. LHCII phosphorylation by a membrane-bound protein kinase leads to the migration of a fraction of LHCII from PSII to PSI by lateral

diffusion in the lipid phase. The LHCII kinase is activated by reduction of plastoquinone (PQ) pool (either by PSII activity or by other cellular metabolic processes) and inactivated by oxidation of PQH_2 by PSI activity. Cytochrome b_6f complex plays a key role in transduction of the redox signal from plastoquinol pool to kinase. Dephosphorylation of Pi-LHCII is catalysed by a phosphatase, which is supposed to be regulated by a 40 kDa luminal protein.

Different authors have proposed that state transitions may be a mechanism of regulation of linear and cyclic electron transports. State 1 and state 2 correspond to two different modes of electron transfer in the green algae *Chlamydomonas reinhardtii* [11,12]. In state 1, PSII and PSI are functionally connected through the linear electron transfer chain, which generates NADPH and ATP. Upon transition from state 1 to state 2, redistribution of LHCII from PSII to PSI and migration of a fraction of the cytochrome b_6f complex from the grana to the stroma thylakoid region induce cyclic electron flow around PSI at the expense of the linear electron flow and, thus, generating solely ATP [12].

STR7 is an atrazine-resistant mutant isolated from photosynthetic cell-suspension cultures of soybean, with a single mutation in the chloroplastic *psb*A gene coding for D1 protein of PSII core [13]. This mutation implies the substitution of serine 268 in D1 protein by proline (S268P) and it is different from the S264G or T mutations reported in other herbicide resistant biotypes. The STR7 strain showed some important differences as compared to the wild type (WT): slower growth, reduced oxygen-evolving activity, reduced electron transfer rate between the secondary acceptors Q_A and Q_B, presence of higher amounts of non-Q_B-reducing PSII centres and a larger antenna size [13]. Two other very interesting characteristics of STR7 mutant are its unusual tolerance to high temperatures and its increased sensitivity to light stress [14,15]. Both properties seem to be related to the alteration of lipid composition found in STR7. This mutant strain showed an unusually high content of saturated (and reduced levels of unsaturated) fatty acids in comparison with WT and, consequently, a more rigid thylakoid membrane matrix [14,16]. Changes in fatty acids unsaturation have also been reported for

many other plant atrazine-resistant mutants, however, on the contrary, these mutants displayed higher levels of unsaturated lipids [17-20].

In this article, we report new data on the photosynthetic characteristics of the STR7 atrazine-resistant mutant. Significant alterations in PSII activity, state transitions and balance between linear and cyclic electron flows have been observed.

2. Materials and methods

2.1. Cell growth conditions

Two different cell culture lines from soybean (G*lycine max* L. cv. Corsoy) were used in this study: SB-P line, kindly provided by Prof. J.M. Widholm (Department of Agronomy, University of Illinois at Urbana, USA), here denoted as the WT strain, and STR7 mutant, obtained from SB-P line by selection against s-triazine herbicide [13]. Both cell lines were grown in solid media on 1.5% (w/v) agar plates in KN^1 medium under continuous low light (10 ± 5 μE m^{-2} s^{-1}) at 24ºC and 5% CO_2 atmosphere [21]. Cells grown in liquid culture were maintained in a climate chamber where they were grown at 25ºC under continuous light at 25 μE m^{-2} s^{-1} before the measurements. Just before the assays, both cell lines were suspended in 50 mM Mes-NaOH (pH 6.5) buffer.

2.2. Thermoluminescence measurements

Thermoluminescence (TL) glow curves of soybean cell suspensions were measured using two similar home-built apparatuses designed by Dr. Ducruet (Saclay, France) for luminescence detection from 0ºC to 80ºC (standard TL) and from 10ºC to 160ºC (high temperature thermoluminescence, HTL). A detailed description of these systems can be obtained elsewhere [22,23]. Typically, samples were dark-incubated for 2 min at 20°C, then cooled to 1°C for 1 min and illuminated at the end of this period with different numbers of saturating single turn-over flashes (separated by 1 s) of white light through an optic fibre.

Luminescence emission was recorded while warming samples from 0°C to 80°C at a heating rate of 0.5°C per s (TL) or from 10ºC to 160ºC at a heating rate of 0.1ºC per s (HTL). N_2 gas was flushed on the sample during HTL experiments in order to desiccate samples and prevents any oxidation induced by high temperatures. The instruments were driven by a PC computer, with a specially developed acquisition program [24]. Data acquisition, signal analysis and graphical simulation were performed as previously described [23,24]. 720 nm illumination was performed with a tungsten lamp through a 720 nm cut-off filter (4 μE m^{-2} s^{-1} light intensity).

2.3. $P700^+$ re-reduction kinetics

The redox state of P700 was monitored by measuring the absorption changes at 820 nm using a dual-wavelength detector Walz ED-P700DW-E attached to a PAM-102 fluorimeter (Walz, Germany). Measurements were performed at 20°C by placing a light guide close to a cell colony in agar Petri dishes. Each colony was illuminated for 30 s by a FR light from a Walz 101-FR LED at setting 10 in order to oxidize P700. Re-reduction of $P700^+$ in the dark was then recorded. Decompositions of re-reduction kinetics into exponentials were done with Sigmaplot 8.0 software.

2.4. Fluorescence measurements

Dark-adapted cell suspensions were successively illuminated by red light (PSII light) for 12 min, red light plus far-red light (PSI light) for 12 min, and, finally, by red light alone. Red light (80 μE m^{-2} s^{-1}) was provided by a tungsten halogen lamp through a 650 nm cut-off filter. Far-red light was provided by a FR-101 Walz LED connected to a PAM-102 unit, generally set at intensity 10. Maximum fluorescence yield (F_m) was measured during exposure of cell suspensions to a saturating flash (1 s, 3000 μE m^{-2} s^{-1}) using a pulse amplitude modulation

fluorimeter (Walz, Germany) as described elsewhere [25]. The relative change in fluorescence was calculated as $[(F_{m1}-F_{m2})/F_{m1})]$ x 100.

For fluorescence spectra, cells from 21-day-old cultures were suspended in 50 mM MES-NaOH, pH 6.5, placed in a 3-mm quartz tube and illuminated at 650 nm or 720 nm for 20 min at room temperature with a 1000 W ORIEL 66187 tungsten halogen lamp. Control samples were not exposed to any selective light treatment. All samples were subsequently frozen in liquid nitrogen. Fluorescence spectra were recorded at 77 K by exciting samples with the tungsten halogen lamp and a double 0.22 m SPEX 1680B monochromator. Excitation light was at 470 nm (3.6 nm slit width) and emission was detected from 650 to 800 nm (1.92 nm slit width). Fluorescence was detected through a 0.5 JARREL-ASH monochromator with a Hamamatsu R928 photomultiplier tube. All measurements were corrected from the system response. Chlorophyll fluorescence emission spectra exhibited peaks at 680 nm and 685 nm due to chlorophyll *a* associated to PSII and at 735 nm from chlorophyll *a* molecules associated mainly to PSI. All spectra were normalized at 685 nm.

3. Results

3.1. Thermoluminescence emission bands from Photosystem II

The thermoluminescence emission technique consists in illuminating a photosynthetic sample at a temperature low enough to block charge recombination processes, then revealing the different types of charge pairs as luminescence emission bands by progressive warming (for a review see [22]). Several TL bands originating from different recombination reactions in PSII can be identified and characterized by this method.

In this work, we have studied some of the most relevant TL bands in dark adapted soybean cell suspensions from WT and STR7 cell lines (Fig. 1). Excitation of WT and STR7 cell suspensions with a series of saturating single turn-over flashes at 1ºC induced the appearance of very complex TL glow curves. The light emission curves obtained after

illumination with two flashes were the greatest of the series and are shown in Fig. 1A. These TL signals could be well simulated by two decomposition components with different t_{max} and contributions to the total signal intensity. We assigned the first component to the well-known TL B band originating from the recombination reactions of $S_3Q_B^-$ and $S_2Q_B^-$ charge pairs. We tentatively assigned the second TL component appearing at higher temperatures to the so-called afterglow (AG) TL emission band usually induced by FR illumination [10]. A similar AG band has been observed in pea, *Arabidopsis* and tobacco leaves excited by white light [10,26,27]. The mathematical analysis of these two components allowed us to estimate t_{max} and contribution of B and AG bands to the total signal intensity in WT and STR7 cell lines, respectively. For the B band, we obtained t_{max} values of about 27ºC for both WT and STR7, and signal contributions of 22% (WT) and 28% (STR7). For the AG band, t_{max} values of 46ºC (WT) and 43ºC (STR7) and signal contributions of 78% (WT) and 72% (STR7) were obtained. These results show two effects of the mutation: (1) a downshift of about 3ºC for AG band; (2) a slight decrease in the ratio between the intensities of the AG and B bands (from 3.5 in WT to 2.6 in STR7).

Analysis of TL yield in dark-adapted samples illuminated by a train of short saturating flashes allows the estimation of the ratio S_0:S_1 and Q_B:Q_B^- in PSII [22,23]. These experiments showed no differences between WT and STR7 cell lines (data not shown), both of them exhibiting a typical four-oscillation period with maxima after the 2^{nd} and 6^{th} flashes for B and AG bands and ratios of 25:75% and 50:50% for S_0:S_1 and Q_B:Q_B^-, respectively.

AG band induced by illumination with white light flashes totally disappeared after incubation of both type of cells (WT and STR7) with 10 μM antimycin (Fig. 1A, inset), a well-known inhibitor of the FQR pathway of cyclic electron transport around PSI [2]. This result suggests that most of electrons leading for AG emission in soybean cells are transferred from the stroma to Q_B via FQR pathway.

To confirm that the proposed AG band observed in soybean cell suspensions after white light flash excitation can be identified as a typical AG band (normally induced by FR light), we have also performed TL measurements after continuous illumination of cell samples with 720 nm (FR) monochromatic light (Fig. 1B). After this illumination, we also excited samples with two white light flashes to ensure induction of maximal signals for B and AG bands. FR illumination generated a more prominent AG band in WT cells, while the B band was reduced. However, for STR7 cells, the intensity pattern was similar to that observed in white light excitation experiments (Fig. 1A). FR light preferentially excites PSI and consequently oxidizes the plastoquinone pool, thus favouring in the dark a back transfer of electrons from stromal reductants to the oxidized Q_B and finally to the S_2 and S_3 states of the manganese cluster [9]. This overall recombination reaction leads to AG emission. Interestingly, FR excitation does not increase the amount of AG band in STR7 mutant. The mathematical analysis of the two components found by the simulation software showed a slight upshift for the B band (t_{max} of 26ºC for WT and 28ºC for STR7), a significant downshift of about 4ºC for the AG band (t_{max} of 46ºC for WT and 42º C for STR7) and an important decrease in the ratio between the intensities of AG and B bands from 4.5 (WT) to 2.3 (STR7). These results support that the 46ºC-band observed in soybean cell suspensions after excitation with white light flashes corresponds to the same recombination reaction which gives rise to the FR-induced AG TL band described in [10]. They also confirm the AG band downshift observed in STR7 TL curves generated by white light flashes (Fig. 1A). A similar AG band downshift has been detected in maize leaves when PSI cyclic electron flow is induced [8].

In order to study recombination reactions involving Q_A, TL band emissions obtained after flashing WT and STR7 soybean cell suspensions previously incubated in the presence of 50 μM DCMU have been recorded (Fig. 1C). In these samples after one flash of white light, the B and AG bands completely disappeared and two other TL bands were detected: (1) at low temperatures, a well-known Q band corresponding to the $S_2Q_A^-$ recombination; and (2), at

high temperatures, a small band with a t_{max} above 60°C that could be assigned to the C band, corresponding to $Tyr_D^+Q_A^-$ recombination [22]. The Q band showed a significant upshift of about 5ºC in STR7 cells (t_{max} of 4ºC) as compared to WT cells (t_{max} of 9ºC).

3.2. Evaluation of lipid peroxidation by high temperature thermoluminescence

Lipid peroxidation status has been studied in both WT and STR7 cells by using the high temperature thermoluminescence emission technique (see Materials and Methods section). Several luminescence high temperature bands (HTL bands) have been observed without prior illumination at temperatures above 60°C [28]. A broad HTL band centred near 130°C (known as the HTL2 band) is generated because of the thermal radiative decomposition of lipid peroxides that, in turn, leads to the formation of carbonyl groups in a triplet state followed by migration of excitation energy toward chlorophylls [28]. It has been demonstrated that this band is indicative of oxidative damage in stressed plants [28,29]. The amplitude of this band has been well correlated with the accumulation of malondialdehyde, an indicator of lipid peroxidation in standard chemical tests [28]. Consequently, HTL2 measurements have been used to study lipid peroxidation in plants subjected to various photooxidative stress conditions [30,31]. Fig. 2 shows that the STR7 mutant presented a very intense HTL2 band (t_{max} at 135º C) in comparison with WT, suggesting a high level of lipid peroxidation in thylakoid membranes of STR7 cells.

3.3. Monitoring cyclic electron flow by $P700^+$ re-reduction kinetics

Cyclic electron flow was examined in both WT and STR7 mutant soybean cells by measuring the kinetics of $P700^+$ reduction after FR excitation [32]. FR light illumination caused the oxidation of P700, monitored as an absorbance increase at 820 nm (data not shown). $P700^+$ re-reduction was then followed by measuring the absorbance decay at 820 nm after turning off the FR light (decay traces in Fig. 3). The kinetic of these absorption changes

included two main exponential components. Bi-exponential decay parameters are in agreement with those determined in C3 and maize plants for a similar electron transfer reaction [1,8,33]. The fast component (about 90% of the total amplitude) decayed with half-lives of 1.52 and 0.45 s in WT and STR7 mutant, respectively, whereas for the slow component, half-lives were 3.35 s (WT) and 3.11 s (STR7) (Table 1). These results show that the overall reduction kinetics of $P700^+$ was much faster in STR7 cells than in WT, suggesting that cyclic electron transfer is activated in this mutant [8].

3.4. State transitions

Two different kinds of fluorescence measurements were performed in order to detect differential changes in PSII fluorescence when WT and STR7 cells are exposed alternatively to light favouring PSII or PSI excitation (Fig. 4). The main objective of these experiments was to determine whether the state transitions process is affected in STR7 mutant. Modulated fluorescence measurements at room temperature have been carried out as described elsewhere [25] (see also Materials and Methods section). Cell suspensions were first illuminated with red light (λ = 650 nm) in order to excite preferentially PSII and, consequently, to stimulate state 2 conditions, and the stationary fluorescence yield was then recorded. After 12 min of red light, cells were additionally illuminated with FR light (λ = 720 nm), leading to stimulation of PSI and, consequently, transition to state 1. Maximal fluorescence in state 1 (F_{m1}) was determined after 12 min of red and FR treatment. Then, FR light was switched off to promote the return to state 2 under red light excitation, and after 12 min, maximal fluorescence in state 2 (F_{m2}) was determined. Transition from state 1 to state 2 can be measured by analyzing the relative changes in maximal fluorescence as $[(F_{m1} - F_{m2})/F_{m1}] \times 100$. This value was 15% in the WT (Fig. 4A, upper part) and almost undetectable (about 3%) in the STR7 mutant (Fig. 4A, lower part).

Low–temperature fluorescence emission spectra at 77 K were also measured in both kinds of cells under conditions promoting either state 1 or state 2 (Fig. 4B). Fluorescence emission spectra at 77 K of soybean cell suspensions displayed three characteristic peaks, two of them corresponding to light re-emitted from PSII at 685 nm (F685) and 695 (F695) and the third one, from PSI in 730-740 nm region (F738). Fluorescence emission spectra of white light-adapted cells from both WT and STR7 strains without any selective light treatment were identical (data not shown) to those obtained in samples after irradiation with 650 nm light (Fig. 4B, light 2, solid line). This result suggests that WT and STR7 cells were in the state 2 under both white light illumination and after 650 nm light excitation. In WT cells, a transition from state 2 to state 1 induced by illumination with 720 nm light was accompanied by a large decrease in relative PSI fluorescence at 738 nm, indicating a redistribution of light excitation energy from PSI to PSII (Fig. 4B, upper part, light 1, dotted line). In contrast, no decrease in relative PSI fluorescence occurred in STR7 mutant after the same light treatment, suggesting that transition from state 2 to state 1 did not occur (Fig. 4B, lower part, light 1, dotted line).

The ratio of fluorescence yield between the two peaks (F685/F738) of 77 K fluorescence spectra depends of the amount of chlorophyll-containing LHC connected to each of the two photosystems. A high F685/F738 ratio indicates that maximal amounts of antenna is associated to PSII (state 1), whereas a low value means the opposite (state 2). White light-adapted WT and STR7 mutant soybean cells had a F685/F738 ratio of about 0.3 and this value was similar upon irradiation with 650 nm light (Table 2). These data are consistent with the assumption that both WT and STR7 cells were in state 2 under conditions of white light or 650 nm light. Transferring light-adapted WT cells (state 2) to 720 nm light illumination conditions caused an increase in the F685/F738 ratio (0.38) indicating a rapid return towards state 1. However, for STR7 cells, the fluorescence F685/F738 ratio did not change significantly between the state induced by both white-light adaptation or after 650 nm

light illumination (0.31) and the state after excitation with 720 nm light (0.29). Thus, the STR7 mutant cells seemed to be partially blocked in state 2 with the LHCII antenna preferentially connected to PSI. The slightly negative value of state transition obtained for STR7 can be interpreted as a non-functional state transition process, while then positive value obtained for the WT reflects a functional state transition (Table 2).

4. Discussion

STR7 is an atrazine-resistant mutant isolated from photosynthetic cell suspension cultures of soybean that has previously shown important physiological differences with respect to WT cells [13-16]. This work reports new data on alterations in photosynthetic activity of the STR7 mutant, mainly concerning PSII activity, state transitions and balance between linear and cyclic electron flows.

Spontaneous mutations of the gene encoding the D1 protein generated in atrazine-resistant plants seem to influence both atrazine- and plastoquinone binding in the Q_B-binding niche of D1 protein, thus affecting PSII activity. Several effects of the STR7 mutation on PSII activity have already been reported: reduced oxygen-evolving activity, reduced electron transfer rate between the secondary acceptors Q_A and Q_B and presence of a higher amount of non-Q_B-reducing PSII centres [13]. In this work, TL emission experiments have shown that this mutation significantly alters the properties of $S_2Q_A^-$ recombination reaction (Fig. 1C). The observed shifting of the Q band toward higher temperatures (about 4ºC) suggests a higher stabilization for $S_2Q_A^-$ charge pair in comparison with WT. Similar charge pair stabilization has been reported for other strains containing mutations in the D-E loop of D1 or lacking the 33-kD protein of the oxygen evolving complex [34, 35]. This change in the energetics of $S_2Q_A^-$ recombination reaction may be explained by a modification of redox potential of the Q_A/Q_A^- couple, which may render the Q_A^- re-oxidation more difficult. No clear effects of the

mutation on the redox properties of Q_B can be inferred from our TL experiments (Fig. 1A and 1B).

It has been shown that fluorescence decay kinetics after one saturating flash was slower in the STR7 mutant than in WT [13]. These experiments showed that electron transfer from Q_A^- to Q_B was slower and that the apparent equilibrium constant between $Q_A^-Q_B$ and $Q_AQ_B^-$ was shifted to $Q_A^-Q_B$. This was explained both by a change in redox potential of Q_A and/or Q_B and by a decrease in Q_B binding. A consequence of this would be a longer lifetime of Q_A^- leading to an increase in its population size. F_0 values, obtained in fluorescence experiments at room temperature, were significantly higher in the mutant as compared to WT (data no shown), lending support to this proposal. Slower rates of electron transfer from Q_A^- to Q_B have also been observed in atrazine-resistant biotypes of several plant species [19,36,37] and in some strains of *Synechocystis* 6714 carrying mutations in the Q_B pocket [38].

Atrazine-resistant mutants including the STR7 strain are more easily photoinhibited [13,37]. A slower electron transfer from Q_A^- to Q_B causes the over-reduction on PSII acceptor side, and consequently, an increased probability of generating reactive oxygen species that can damage membrane components. The larger antenna size observed in this mutant may also explain the increase of the photoinactivation processes in PSII. One of the damaging effects of reactive oxygen species (mostly singlet oxygen) is lipid peroxidation in thylakoid membranes, that can be probed by monitoring the high temperature TL band HTL2, peaking around 130°C. Analysis of HTL2 bands obtained from WT and STR7 cells (Fig. 2) clearly showed a much higher level of lipid peroxidation in STR7. These results suggest high rate of generation of reactive oxygen species in the STR7 mutant. We propose that the slower electron transfer from Q_A^- to Q_B induced by STR7 mutation increases the probability of generating singlet oxygen in PSII, which may initiate the lipid peroxidation process in thylakoid membranes.

Measurements of $P700^+$ reduction kinetics after FR illumination indicated that a cyclic pathway provides electrons faster to PSI in STR7 in comparison with WT (Fig. 3). The

significant downshift of the AG band observed in the mutant (Fig. 1) also suggests that a cyclic/chlororespiratory pathway would be permanently operative, so that the backflow of electrons towards $S_{2/3}Q_B$-centres generating this band occurs at lower temperatures [5,8]. These results allow us to propose that in the STR7 mutant the cyclic electron transport is active under normal growth conditions. The STR7 mutant has a reduced PSII capacity and, thus, it is likely to develop a compensatory mechanism for maintenance of a normal photosynthetic activity. The correlation of an inhibition of linear electron flow with an activation of cyclic electron transfer pathway around PSI has already been proposed [39].

State transitions measured by changes in maximal fluorescence (Fig 4A) when cells are exposed alternatively to light favouring PSII excitation and light favouring PSI excitation were hardly detectable for the STR7 mutant. Low-temperature fluorescence emission spectra measured at 77 K indicated that in the mutant there is no transition from state 2 to state 1. These results demonstrated that the STR7 mutant is defective in state transitions and that it is probably locked in state 2. It has been proposed that state transitions may be a mechanism of regulation of linear and cyclic electron transport [11,12]. In state 2, redistribution of the LHCII antenna from PSII to PSI and migration of a fraction of cytochrome b_6f complex from the grana to the stroma lamellae induce cyclic electron flow around PSI. Our results suggest a correlation between permanent operation of cyclic electron transport in STR7 mutant and its presence in state 2.

The results of this work show that the STR7 mutant is in state 2 under all illumination conditions tested, including that inducing state 2 to state 1 transition (i.e. 720 nm light) (Fig. 4). State transitions reflect the reversible association of part of the LHCII with either PSII (in state 1) or PSI (in state 2) depending on the redox state of the intersystem electron carriers. However, fluorescence induction experiments did not show any significant differences in the redox state of plastoquinone pool between WT and STR7 mutant cells (data not shown). In plants, the movement of LHCII depends on its phosphorylation [40]. However, our results do

not suggest any reason why LHCII could not be phosphorylated or dephosphorylated in the mutant. Thus, the only possible explanation to understand why the state transitions are blocked in the mutant is that there is no movement of the dephosphorylated LHCII from PSI towards PSII. As already mentioned in this paper, the thylakoid membrane of the STR7 mutant is more rigid than that of the WT [14, 16]. An increase in the thylakoid membrane rigidity could be responsible for locking the STR7 cells in state 2 due to impaired lateral diffusion of protein complexes. A similar conclusion was obtained when state transitions were studied in cyanobacterial mutants defective in thylakoid membrane unsaturation [41]. The analysis of *Arabidopsis* mutants defective in thylakoid membrane unsaturation, lacking mutations in the *psbA* gene [42], may help to clarify this mechanism.

It is more difficult to understand why a point mutation in the PSII D1 protein induces such changes. The plant ω3 fatty-acid desaturases FAD7, FAD8 and FAD3 are responsible for the production of trienoic fatty-acid. Their activities are responsible for the maintenance of appropriate thylakoid membrane fluidity. The expression of these enzymes seems to be regulated in response to light [43] and to photosynthetic electron transport activity (Collados, Picorel and Alfonso, unpublished observations) in soybean cells. Studies are in progress in our laboratory to further test this hypothesis.

Acknowledgements

This work was supported by grants from the Ministry of Education and Culture of Spain (BFU-BMC2004-04914-C02-01, BMC2002-00031 and BFU-BMC2005-07422-C02-01) and Andalusia Government (PAI CVI-261). The authors thank Dr. J.R. Pérez-Castiñeira and Dr. A.M. Lindahl for critical reading of the manuscript. We also thank M.V. Ramiro for helpful technical assistance and Dr. R. Cases (ICMA-CSIC) for help in fluorescence spectra measurements.

References

[1] N. Bukhov, R. Carpentier, Alternative photosystem I-driven electron transport routes: mechanisms and functions, Photosynth. Res. 82 (2004) 17-33.

[2] D.S. Bendall, R.S. Manasse, Cyclic photophosphorylation and electron transport, Biochim. Biophys. Acta 1229 (1995) 23–38.

[3] H.V. Scheller, In vitro cyclic electron transport in barley thylakoids follows two independent pathways, Plant Physiol. 110 (1996) 187–194.

[4] T. Shikanai, T. Endo, T. Hashimoto, Y. Yamada, K. Asasa, A. Yokota, Directed disruption of the tobacco *ndhB* gene impairs cyclic electron flow around photosystem I, Proc. Natl. Acad. Sci. USA 95 (1998) 9705–9709.

[5] M. Havaux, D. Rumeau, J.-M. Ducruet, Probing the FQR and NDH activities involved in cyclic electron transport around Photosystem I by the "afterglow" luminescence, Biochim. Biophys. Acta 1709 (2005) 203–213.

[6] H. Nakamoto, L.-G. Sundblad, P. Gardeström, E. Sundbom, Far-red stimulated long-lived luminescence from barley protoplasts, Plant Sci. 55 (1988) 1– 7.

[7] M. Havaux, Short-term responses of photosystem I to heat stress. Induction of a PSII-independent electron transport through feed by stromal components, Photosynth. Res. 47 (1996) 85- 97.

[8] J.-M. Ducruet, M. Roman, M. Havaux, T. Janda, A. Gallais, Cyclic electron flow around PSI monitored by afterglow luminescence in leaves of maize inbred lines (*Zea mays* L.): correlation with chilling tolerance, Planta 221 (2005) 567–579.

[9] L.G. Sundblad, W.P. Schröder, H.-E. Åkerlund, S-state distribution and redox state of Q_A in barley in relation to luminescence decay kinetics, Biochim. Biophys. Acta 973 (1988) 47–52.

[10] T. Miranda, J.-M. Ducruet, Characterization of the chlorophyll thermo-luminescence afterglow in dark-adapted or far-red-illuminated plant leaves, Plant Physiol. Biochem. 33 (1995) 689-699.

[11] F.-A. Wollman, State transitions reveal the dynamics and flexibility of the photosynthetic apparatus, EMBO J. 20 (2001) 3623–3630.

[12] G. Finazzi, The central role of the green alga *Chlamydomonas reinhardtii* in revealing the mechanism of state transitions, J. Exp. Bot. 56 (2005) 383–388.

[13] M. Alfonso, J.J. Pueyo, K. Gaddour, A.-L. Etienne, D. Kirilovsky, R. Picorel, Induced new mutation of D1 serine-268 in soybean photosynthetic cell cultures produced atrazine resistance, increased stability of S_2Q_B and S_3Q_B states, and increased sensitivity to light stress, Plant Physiol. 112 (1996) 1499–1508.

[14] M. Alfonso, I. Yruela, S. Almárcegui, E. Torrado, M.A. Pérez, R. Picorel, Unusual tolerance to high temperatures in a new herbicide-resistant D1 mutant from *Glycine max* (L.) Merr. cell cultures deficient in fatty acid desaturation, Planta 212 (2001) 573–582.

[15] M. Alfonso, R. Collados, I. Yruela, R. Picorel, Photoinhibition and recovery in a herbicide-resistant mutant from *Glycine max* (L.) Merr. cell cultures deficient in fatty acid unsaturation, Planta 219 (2004) 428-439.

[16] I. Yruela, M. Alfonso, I. García-Rubio, J.I. Martinez, R. Picorel, P.J. Alonso, Spin label electron paramagnetic resonance study in thylakoid membranes from a new herbicide-resistant D1 mutant from soybean cell cultures deficient in fatty acid desaturation, Biochim. Biophys. Acta 1515 (2001) 55–63.

[17] P. Pillai, J.B. St John, Lipid composition of chloroplast membranes from weed biotypes differentially sensitive to triazine herbicides, Plant Physiol. 68 (1981) 585-587.

[18] Y. Lemoine, J.P. Dubacq, G. Zabulon, J.-M. Ducruet, Organization of the photosynthetic apparatus from triazine-resistant and susceptible biotypes of several plant species, Can. J. Bot. 64 (1986) 2999–3007.

[19] R. De Prado, C. Dominguez, I. Rodríguez, M. Tena, Photosynthetic activity and chloroplast structural characteristics in triazine-resistant biotypes of three weed species, Physiol. Plant. 84 (1992) 477–485.

[20] C. Schwenger-Erger, W. Barz, N. Weber, Fatty acid alteration of plastidic and extra-plastidic membrane lipids in metribuzin-resistant photoautotrophic *Chenopodium rubrum* cells as compared to wild type cells, Z. Natursforch. 56 (2001) 1047–1056.

[21] M. Bernal, P.S. Testillano, M.C. Risueño, I. Yruela, Excess copper induces structural changes in cultured photosynthetic soybean cells, Funct. Plant Biol. 33 (2006) 1001-1012.

[22] J.-M. Ducruet, Chlorophyll thermoluminescence of leaf discs: simple instruments and progress in signal interpretation open the way to new ecophysiological indicators, J. Exp. Bot. 54 (2003) 2419-2430.

[23] J.L. Zurita, M. Roncel, M. Aguilar, J.M. Ortega, A thermoluminescence study of Photosystem II back electron transfer reactions in rice leaves – efects of salt stress. Photosynth. Res. 84 (2005) 131–137.

[24] J.M. Ducruet, T. Miranda, Graphical and numerical analysis of thermoluminescence and fluorescence F_0 emission in photosynthetic material. Photosynth. Res. 33 (1992) 15-27.

[25] S. Bellafiore, F. Barneche, G. Peltier, J.-D. Rochaix, State transitions and light adaptation require chloroplast thylakoid protein kinase STN7, Nature 24 (2005) 892-895.

[26] M. Roncel, J.M. Ortega, Afterglow thermoluminescence band as a possible early indicator of changes in the photosynthetic electron transport in leaves, Photosynth. Res. 84 (2005) 167-172.

[27] J.-M. Ducruet, M. Roman, J.M. Ortega, T. Janda, Role of the oxidized secondary acceptor Q_B of photosysthem II in the delayed "afterglow" chlorophyll luminescence, Photosynth. Res. 84 (2005) 161-166.

[28] D.V. Vavilin, J.-M. Ducruet, The origin of 115-130°C thermoluminescence bands in chlorophyll-containing material, Photochem. Photobiol. 68 (1998) 191-198.

[29] M. Havaux, K.K. Niyogi, The violaxanthin cycle protects plants from photooxidative damage by more than one mechanism, Proc. Natl. Acad. Sci. U. S. A. 96 (1999) 8762–8767.

[30] I. Baroli, B.J. Gutman, H.K. Ledford, J.W. Shin, B.L. Chin, M. Havaux, K.K. Noyogi, Photo-oxidative stress in xanthophylls-deficient mutant of *Chlamydomonas*, J. Biol. Chem. 279 (2004) 6337-6344.

[31] M.N. Merzlyak, V.K. Pavlov, T.V. Zhigalova, Effect of desiccation on chlorophyll high temperature chemiluminescence in *Acer platanoides* L. and *Aesculus hippocastanum* L. leaves, J. Plant Physiol. 139 (1992) 629-631.

[32] U. Schreiber, C. Klughammer, C. Neubauer, Measuring P700 absorbance changes around 830 nm with a new type of pulse modulation system, Z. Naturforsch 43c (1988) 686-698.

[33] G. Cornic, N.G. Bukhov, C. Wiese, R. Bligny, U. Heber, Flexible coupling between light-dependent electron and vectorial proton transport in illuminated leaves of C3 plants. Role of photosystem I-dependent proton pumping, Planta 210 (2000) 468-477.

[34] P. Mäenpää, T. Miranda, E. Tyystjarvi, T. Tyystjarvi, Govindjee, J.-M. Ducruet, A.-L. Etienne, D. Kirilovsky, A mutation in the D-*de* loop D1 modifies the stability of the $S_2Q_A^-$ and $S_2Q_B^-$ states in photosystem II, Plant Physiol. 107 (1995) 187-197.

[35] R. Burnap, J.-R. Shen, P. Jursinic, Y. Inoue, L. Sherman, Oxygen yield and thermoluminescence characteristics of a cyanobacterium lacking the manganese-stabilizing protein of photosystem II, Biochemistry 31 (1992) 7404-7410.

[36] A.-L. Etienne, J.-M. Ducruet, G. Ajlani, C. Vernotte, Comparative studies on electron transfer in photosystem II of herbicide-resistant mutants from different organisms, Biochim. Biophys. Acta 1015 (1990) 435-440.

[37] C. Sundby, W.-S. Chow, J.M. Anderson, Effects on photosystem II function, photoinhibition, and plant performance of the spontaneous mutation of Serine-264 in the photosystem II reaction center D1 protein in triazine-resistant *Brassica napus* L., Plant Physiol. 103 (1993) 105-113.

[38] I. Perewoska, A.L. Etienne, T. Miranda, D. Kirilovsky, S1 destabilization and higher sensitivity to light in metribuzin-resistant mutants, Plant Physiol. 104 (1994) 235-245.

[39] A.J. Golding, G.N. Johnson, Down-regulation of linear and activation of cyclic electron transport during drought, Planta 218 (2003) 107-114.

[40] A.V. Vener, P.J.M. van Kan, P.R. Rich, B. Andersson, I. Ohad, Plastoquinol at the quinol oxidation site of reduced cytochrome bf mediates signal transduction between light and protein phosphorylation: thylakoid protein kinase deactivation by a single-turnover flash, Proc. Natl. Acad. Sci. U. S. A. 94 (1997) 1585-1590.

[41] K. El Bissati, E. Delphin, N. Murata, A.L. Etienne, D. Kirilovsky, Photosystem II fluorescence quenching in the cyanobacterium *Synechocystis* PCC 6803: involvement of two different mechanisms, Biochim. Biophys. Acta 1457 (2000) 229-242.

[42] Wallis, J.G. and Browse, J. (2002) Mutants of Arabidopsis revelal many roles of membrane lipids. Prog. Lipid Res. 41(2002) 254-278.

[43] R. Collados, V. Andreu, R. Picorel, M. Alfonso, A light-sensitive mechanism differently regulates transcription and transcript stability of omega3 fatty-acid desaturases (FAD3, FAD7 and FAD8) in soybean photosynthetic cell suspensions, FEBS Lett. 580 (2006) 4934-4940.

Figure legends

Figure 1. (A) Thermoluminescence glow curves from soybean cells of WT and STR7 lines recorded after two flashes. The dashed lines represent the simulation components corresponding to the best fit (see Materials and Methods). *Inset*: TL signal recorded after two flashes from WT and STR7 soybean cells incubated in the presence of antimycin. Dark-adapted cell suspensions were incubated for 5 min in the dark at room temperature with 10 μM antimycin. (B) Thermoluminescence glow curves from WT and STR7 mutant soybean cells recorded after two flashes with previous illumination with 720 nm monochromatic light. Cells resuspended in 50 mM Mes-NaOH, pH 6.5 buffer were dark-adapted for 2 min at 20ºC and then irradiated 5 min with 720 nm light at 20ºC, and subsequently cooled to 0ºC during 1 min. Two flashes were given at the end of this period. The dashed lines represent the simulation components corresponding to the best fit (see Materials and Methods). (C) Thermoluminescence glow curves after one flash of WT and STR7 cells previously incubated in the presence of DCMU. Dark-adapted cell suspensions were incubated in darkness at room temperature with 50 μM DCMU.

Figure 2. HTL measurements recorded from 10ºC to 160ºC from WT and STR7 mutant soybean cells. Only the 70-160ºC range of the HTL bands is shown. Samples were dark-adapted for 1 min at 10ºC and heated with a slow warming rate of 0.1 ºC/s from 10ºC to 160ºC without flash excitation. In order to desiccate the samples and prevent any oxidation induced by high temperature, N_2 was flushed on the samples during the HTL experiments.

Figure 3. Dark re-reduction of $P700^+$ in soybean cells of WT and STR7 mutant. $P700^+$ reduction was measured by monitoring absorbance changes at 830 nm in the dark after oxidation induced by a 30-s pulse of FR light. The measurements were made directly on

single colonies in agar Petri plates at 20ºC. Experimental data are shown as open circles and the lines represent the biexponential fitted curves.

Figure 4. (A) Measurements of transitions between state 1 and state 2 in WT and STR7 mutant soybean cells. Dark-adapted cells were exposed either to light favouring PSII excitation (650 nm monochromatic light) or light favouring PSI excitation (720 nm monochromatic light). The fluorescence decreases when illumination includes PSI light and increases again when illumination is changed to favour PSII. (B) 77 K fluorescence emission spectra of WT and STR7 mutant cells incubated under light 2 (Solid line) and light 1 (dotted lines) for 20 min immediately prior to freezing at 77 K. Light 2, 650 nm monochromatic light; Light 1, 720 nm monochromatic light. All spectra were normalized at 685 nm.

Table 1. Kinetic parameters of $P700^+$ dark reduction in soybean STR7 mutant and WT cells.

	Fast phase		Slow phase
	Amplitude (%)	$t_{½}$ (s)	$t_{½}$ (s)
WT	90 ± 4	1.52 ± 0.07	3.35 ± 0.50
STR7	89 ± 5	0.45 ± 0.06	3.11 ± 1.01

Experimental conditions were described in Materials and Methods. Amplitudes and half-lives were calculated according to a biexponential curve fit. Data are the means ± SD of five independent experiments.

Table 2. Measurements from 77 K fluorescence emission spectra of soybean STR7 mutant and WT cells.
Mean ± SD, *n* = 3

Light treatment	F685/F738[1] WT	F685/F738 STR7
Light adapted[2]	0.29 ± 0.008	0.31 ± 0.005
650 nm	0.28 ± 0.007	0.31 ± 0.006
720 nm	0.38 ± 0.009	0.29 ± 0.005
State transition[3]	26%	-7%

[1]F685: fluorescence at 685 nm; F738: fluorescence at 738 nm
[2] (10 μE m^{-2} s^{-1})
[3]State transition: $[(F_{685/738}(ox)–F_{685/738}(red))/F_{685/738}(ox)] \times 100$. $F_{685/738}(ox)$ = fluorescence ratio obtained under illumination with 720 nm light; $F_{685/738}(red)$ = fluorescence ratio obtained under illumination with 650 nm light

Fig. 1

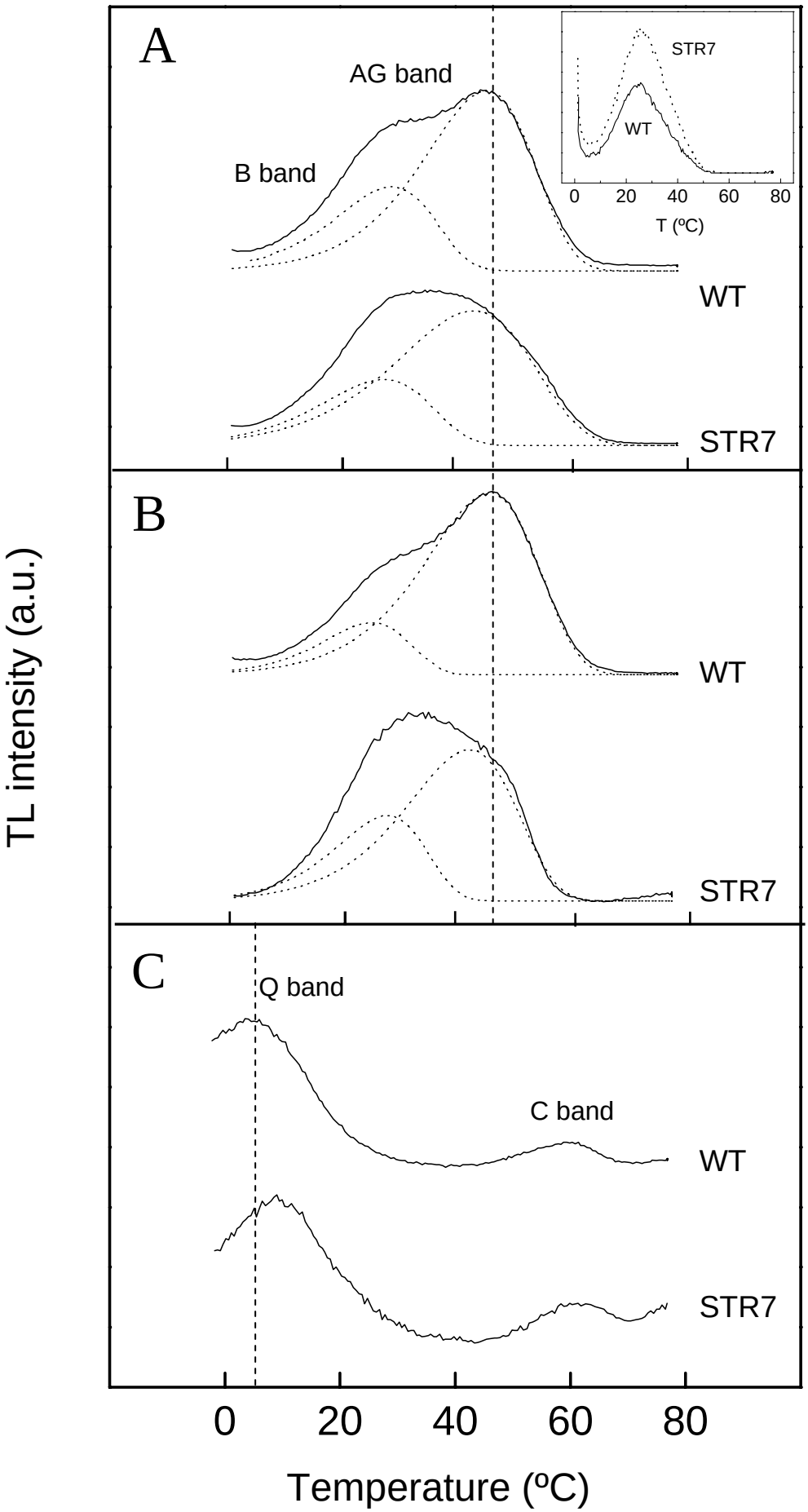
A
AG band
B band
STR7
WT
0
20
40
60
80
T (ºC)
WT
STR7
B
WT
STR7
C
Q band
C band
WT
STR7
TL intensity (a.u.)
0
20
40
60
80
Temperature (ºC)

Fig. 2

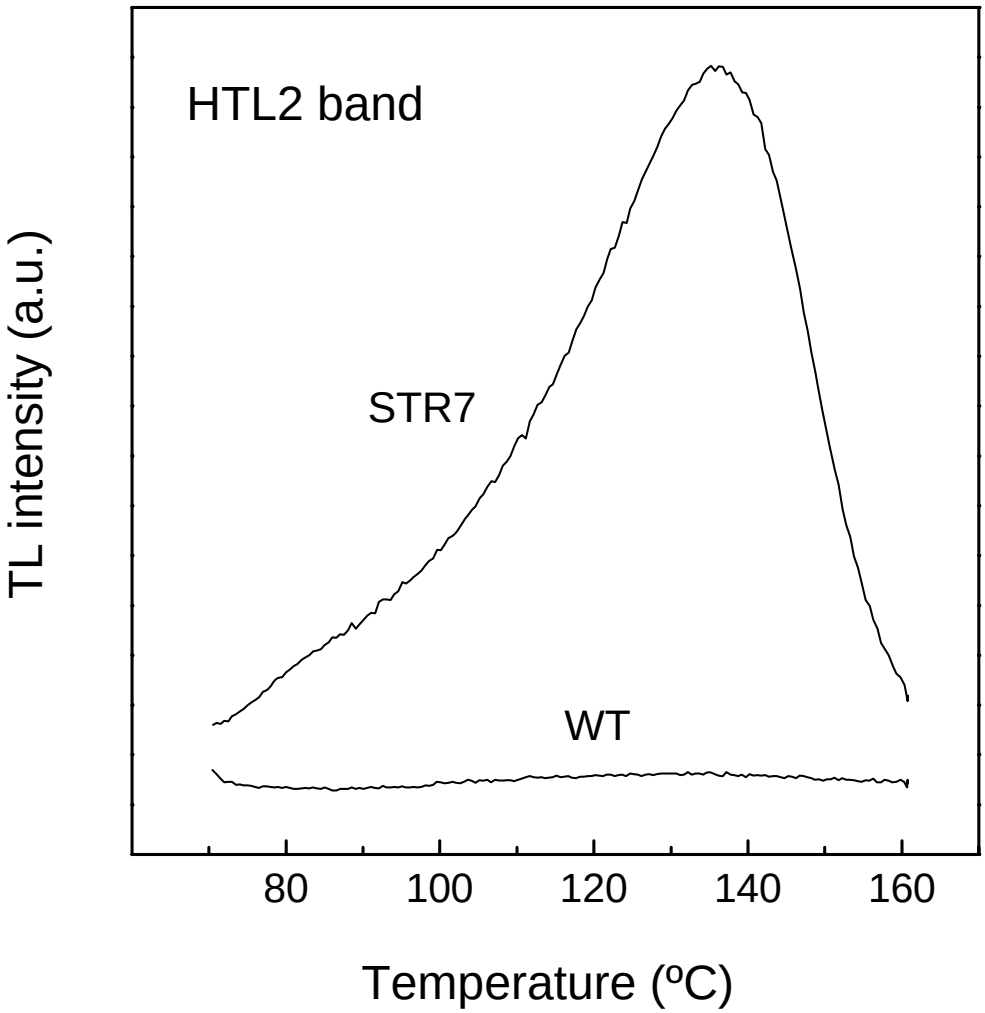
HTL2 band
STR7
WT
TL intensity (a.u.)
80
100
120
140
160
Temperature (ºC)

Fig. 3

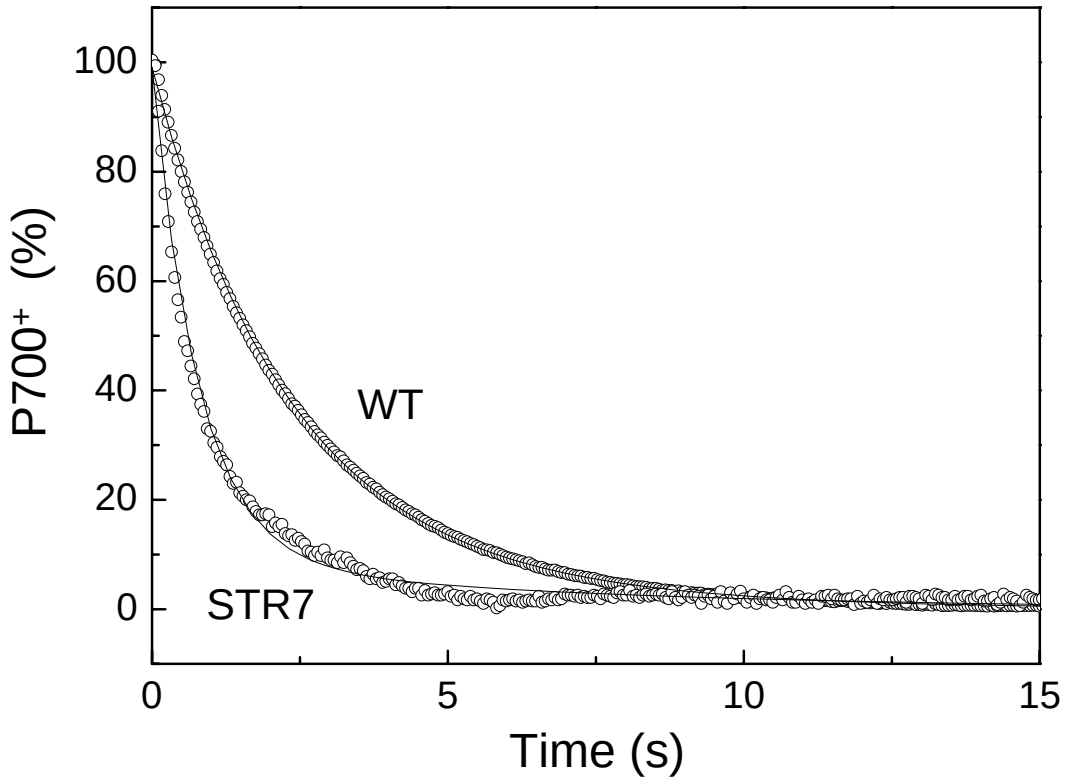

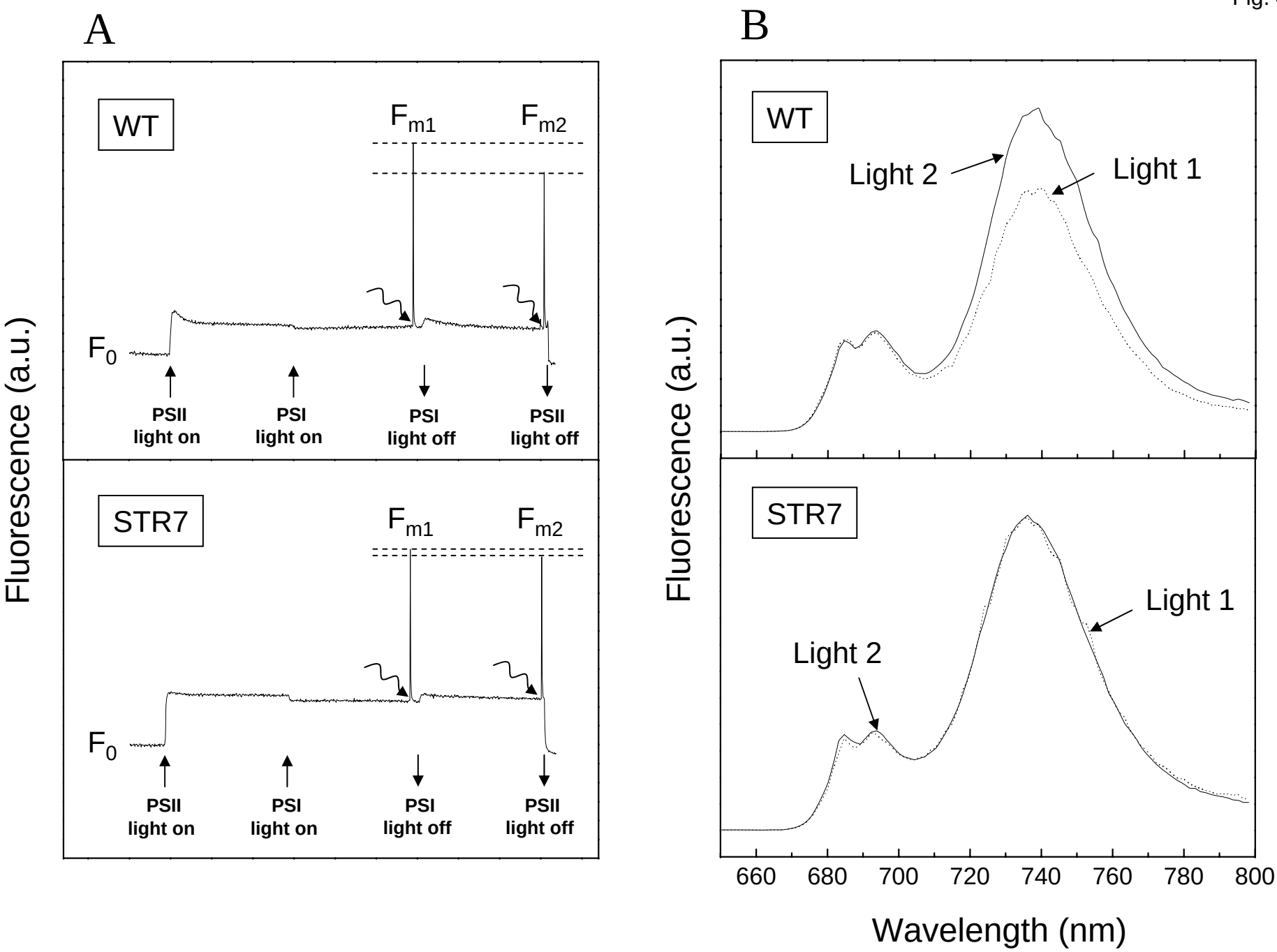
A
WT
F_{m1}
F_{m2}
F_0
PSII light on
PSI light on
PSI light off
PSII light off
STR7
F_{m1}
F_{m2}
F_0
PSII light on
PSI light on
PSI light off
PSII light off
Fluorescence (a.u.)
B
WT
Light 2
Light 1
STR7
Light 2
Light 1
Fluorescence (a.u.)
660
680
700
720
740
760
780
800
Wavelength (nm)